Comparing the structure and dynamics of phospholamban pentamer in its unphosphorylated and pseudo-phosphorylated states

Kirill Oxenoid, Amanda J. Rice and James J. Chou

Protein Sci. 2007 16: 1977-1983
Access the most recent version at doi:10.1110/ps.072975107

Comparing the structure and dynamics of phospholamban pentamer in its unphosphorylated and pseudo-phosphorylated states

KIRILL OXENOID, AMANDA J. RICE, AND JAMES J. CHOU

Department of Biological Chemistry and Molecular Pharmacology, Harvard Medical School, Boston, Massachusetts 02115, USA

(RECEIVED April 27, 2007; FINAL REVISION June 13, 2007; ACCEPTED June 13, 2007)

Abstract

Human phospholamban (PLN), a 30 kDa homopentamer in the sarcoplasmic reticulum (SR) membrane, controls the magnitude of heart muscle contraction and relaxation by regulating the calcium pumping activity of the SR Ca^{2+}-ATPase (SERCA). When PLN is not phosphorylated, it binds and inhibits SERCA. Phosphorylation of PLN at S16 or T17 releases such inhibitory effect. It remains a matter of debate whether phosphorylation perturbs the structure of PLN, which in turn affects its interaction with SERCA. Here we examine by NMR spectroscopy the structure and dynamics of PLN pentamer with a physiologically relevant, phosphorylation-mimicking mutation, S16E. Based on extensive NMR data, including NOEs, dipolar couplings, and solvent exchange of backbone amides, we conclude that the phosphorylation-mimicking mutation does not perturb the pentamer structure. However, ^{15}N R_1 and R_2 relaxation rates and $^{15}N(^1H)$ NOEs suggest subtle differences in the dynamics of the extramembrane portion of the protein.

Keywords: phospholamban pentamer; pseudophosphorylation; NMR

Contraction and relaxation of heart muscle cells is regulated by cycling of calcium between the cytoplasmic and SR compartments. The myocyte relaxes when calcium is pumped from the cytoplasm to the SR by the sarco(endo)plasmic reticulum calcium ATPase, SERCA, and contracts when calcium is released back into the cytoplasm via the ryanodine receptor RyR2 (Zucchi and Ronca-Testoni 1997). PLN is an α helical membrane protein (52 amino acids) that assembles spontaneously into a 30 kDa pentamer in the SR membrane of heart muscle cells (MacLennan and Kranias 2003). It is the main, but not the only regulator of SERCA. In the unphosphorylated form, PLN has an inhibitory effect on the calcium pump, thereby decreasing the magnitude of calcium cycling and muscle contractility. Heart stimulants, such as adrenaline, set off a chain of signal transduction events that among other effects lead to PLN phosphorylation. Phosphorylated PLN no longer inhibits SERCA, allowing for larger muscle contractility.

Substantial progress has been made toward an understanding of this phosphorylation-dependent regulatory mechanism at the atomic resolution. The crystal structure of SERCA is available (Toyoshima and Nomura 2002), and its putative sites of interaction with PLN have been proposed based on a number of chemical cross-linking and mutagenesis experiments (Toyoshima et al. 2003). The solution structures of both the monomeric mutants (Lamberth et al. 2000; Zamoon et al. 2003) and the pentameric wild type (Oxenoid and Chou 2005) of PLN have been determined by NMR spectroscopy. In addition, a recent study reported two-dimensional co-crystallization of the I40A PLN mutant, believed to be monomeric based on SDS-PAGE experiments, and SERCA (Stokes et al. 2006). Although the two-dimensional crystal diffracts poorly to

Reprint requests to: James J. Chou, 250 Longwood Avenue, SGM 109, Boston, MA 02115, USA; e-mail: james_chou@hms.harvard.edu; fax: (617) 432-2921.

Article and publication are at http://www.proteinscience.org/cgi/doi/10.1110/ps072975107.

~17 Å, a low-resolution projection map could be reconstructed. The map unexpectedly reveals PLN densities that are more consistent with the oligomeric form than the monomer, suggesting that SERCA can directly interact with the native pentameric assembly of PLN. Despite this progress, there has not been a high-resolution structure reported of a PLN–SERCA complex from which a definitive mechanism of phosphorylation-dependent regulation can be deduced.

A controversial yet important question concerning PLN structure is whether phosphorylation has an effect on the conformation and how potential structural changes relate to the interaction between PLN and SERCA. Limited proteolysis experiments showed a reduction in the sensitivity of PLN to digestion by proteases after phosphorylating Ser16, suggesting that the PLN pentamer structure becomes more stable upon phosphorylation (Huggins and England 1987). However, more direct measurements using circular dichroism (CD) and Fourier transform infrared (FTIR) methods did not observe any significant changes in the secondary structure of PLN upon phosphorylation (Simmerman et al. 1989; Arkin et al. 1995). Solution NMR studies on the AFA-PLN monomeric mutant (with C36A, C41F, C46A mutations) showed that the helical region near Ser16 (residues 14–21) becomes disordered upon phosphorylation (Metcalfe et al. 2005), whereas a recent solid-state NMR study of the wild-type (WT) PLN in lipid bilayer reported that Ala15 of the extramembrane domain near the phosphorylation site is a part of an α helical structure for both unphosphorylated and phosphorylated PLN (Abu-Baker and Lorigan 2006).

To provide further details of potential structural perturbation of PLN caused by phosphorylation, we compare the structure and dynamics of the WT PLN with its phosphorylation-mimicking mutant that has a S16E substitution. Mutations of serine and threonine to aspartic or glutamic acids are often used to study the effects of protein phosphorylation (Park et al. 2006; Yang et al. 2007). Using adenoviral vector delivery, it has been shown in the mouse model that expression of the S16E mutant causes an increase in muscle contraction and relaxation. Moreover, this effect was no longer dependent on β-adrenergic agonists, mimicking constitutively phosphorylated PLN (Hoshijima et al. 2002). A practical advantage of choosing the S16E mutation over phosphorylation by kinase is to avoid the difficulty of achieving 100% phosphorylation as well as problems of dephosphorylation in the NMR sample over an extended period of time. Extensive NMR measurements including NOEs, residual dipolar couplings (RDCs), and amide-solvent exchange factors indicate that the structure of the S16E mutant is almost identical to that of the WT. R_1 and R_2 relaxation rates and heteronuclear NOEs, however, suggest subtle differences in the chemical exchange and dynamics in the extramembrane domain (residues 1–20) that may have implications in the reduced inhibitory activity of PLN upon phosphorylation.

Results and Discussion

The S16E mutation does not change the pentamer structure

The high-resolution NMR structure of the WT PLN consists of three distinct regions: an extramembrane α helix (residues 2–15), a partially structured and extended linker (residues 16–22), and a transmembrane (TM) coiled-coil domain that holds the pentamer together (Oxenoid and Chou 2005). The phosphorylation sites Ser16 and Thr17 are near the C-terminal end of the extramembrane helix. An intriguing question is whether introducing negative charges at Ser16 and/or Thr17 perturbs the structure of the pentameric assembly.

The ^{1}H-^{15}N TROSY spectra of the WT and the S16E mutant PLN pentamers are compared in Figure 1A. The residue-specific chemical-shift changes are quantified by the chemical-shift distance (δ, normalized to ^{1}H chemical shift) between perturbed resonances, defined as $\delta = \left[(\Delta H)^2 + (\Delta N/\eta)^2\right]^{1/2}$, where η is the ratio of total resonance dispersion of ^{15}N to that of ^{1}H in ppm, and ΔH and ΔN are ^{1}H and ^{15}N chemical-shift changes in ppm, respectively (Fig. 1B). In the case of PLN, pentamer reconstituted in DPC micelles, $\eta = 10$. The resonances corresponding to the membrane-embedded region (residues 23–52) essentially do not change, indicating that the structure of the coiled-coil assembly is not at all affected by the S16E mutation. However, there are chemical-shift perturbations in regions close to the phosphorylation site, with the largest change in residues 13–17, and smaller but significant changes in residues 8–12 and 18–20. The long-range chemical-shift perturbation may be a result of alteration of either structure or dynamics, or both.

To compare the structures more directly, NOEs and ^{1}H-^{15}N residual dipolar couplings (RDCs) have been measured. Short-range NOEs between amino acids that are less than four residues apart were extracted from a 3D ^{15}N-separated NOESY spectrum and are summarized in Figure 2A. The NOE pattern agrees completely with the WT structure, showing that residues 2–15 form a continuous α helix. The structure of the nonhelical region (residues 16–22) connecting the extramembrane α helix and the TM domain is also very similar to that of the WT. In addition, ^{1}H-^{15}N RDCs were measured for the S16E mutant marginally oriented in a stretched polyacrylamide gel and are compared with those previously measured for the WT protein weakly oriented in the same medium. The RDCs from the two proteins agree very well, with a correlation coefficient

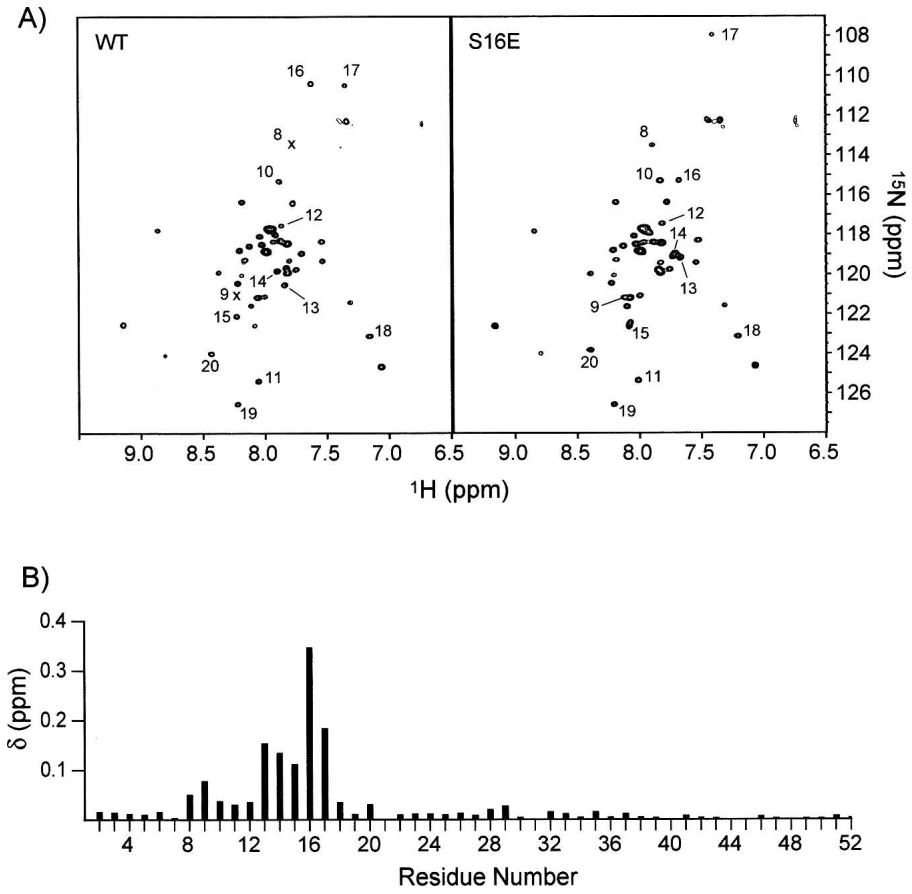

Figure 1. Chemical-shift differences between the WT PLN and the S16E mutant reconstituted in DPC micelles. (*A*) ^{1}H-^{15}N TROSY spectra of ^{15}N-, ^{2}H-labeled WT (*left*) and the mutant (*right*) PLN acquired at 30°C at ^{1}H frequency of 600 MHz. The residues whose chemical shift has significantly changed are labeled. (*B*) Residue-specific chemical-shift difference represented by the (^{1}H, ^{15}N) chemical-shift distance, δ, defined in the text.

of 0.94 (Fig. 2B). Note in Figure 2B that the linear regression line crosses the (0,0) point (considering an error margin of ~0.4 Hz in RDC measurement), indicating that the structures and the alignment tensors of the WT and the mutant are almost identical.

The protection coefficients of the amide protons from exchanging with water are highly informative of membrane protein structure in detergent micelles, because there are typically distinct regions of protein that are either detergent or water exposed. The relative degrees of amide–water exchange provide yet another independent probe for changes in structure and stability of the pentameric assembly. The relative amide protection in the WT and the mutant were obtained by measuring attenuation of the amide resonances due to water saturation. This was accomplished by recording two interleaved TROSY spectra, one in the absence (reference spectrum) and the other in the presence (attenuated spectrum) of 1 sec of presaturation of the water resonance. In order to avoid the complication arising from NOEs due to partial saturation of α and/or β protons, ^{15}N-, ^{2}H-labeled proteins were used along with deuterated detergent. The ratios of peak intensity in the attenuated spectrum (I_{sat}) to that in the reference spectrum (I_{ref}) are shown in Figure 2C. There are essentially no differences in residue-specific I_{sat}/I_{ref} between the WT and the mutant in DPC micelles except for residues 15–17. For these three residues, the differences in attenuation are probably due to NOE from presaturating the OH group of Ser16 in the WT, which is absent in the mutant. The similarity in amide–water exchange factors suggests that the mutation does not affect the local secondary structures, nor does it alter the way the pentamer is assembled in the detergent micelles.

The results of a combined analysis of chemical-shift perturbation, NOEs, RDCs, and amide–water exchange allow us to conclude that there are no detectable differences in both secondary and tertiary structures between the WT and the S16E mutant. Since the S16E mutation is recognized as a pseudophosphorylation mutation (Hoshijima et al. 2002), the above results indicate that the structure of the PLN pentamer is not significantly perturbed upon phosphorylation of Ser16.

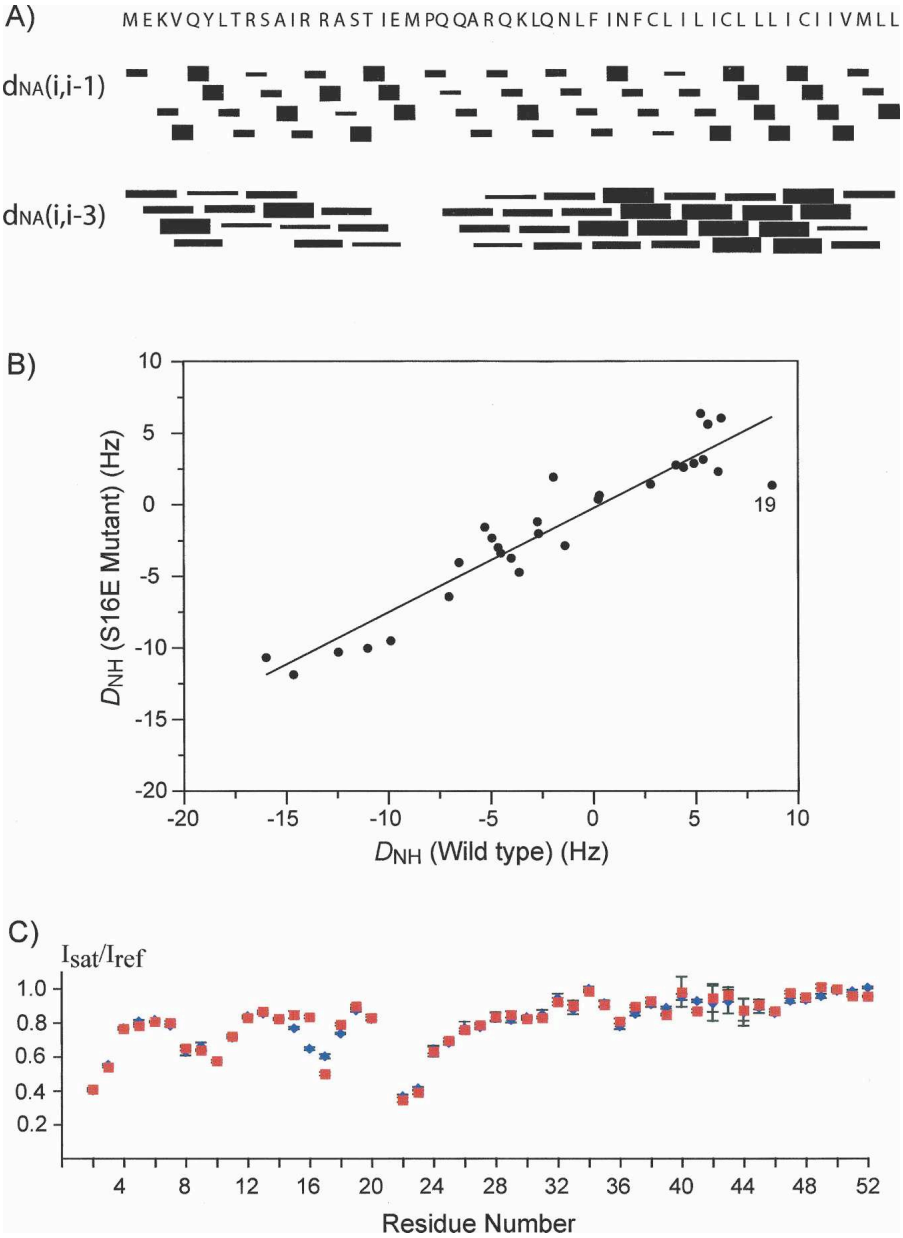

Figure 2. Characterization of the effect of the phosphorylation-mimicking mutation, S16E, on the structure of the PLN pentamer. (*A*) NOEs between $^{1}H^{N}$ of residue *i* and $^{1}H^{\alpha}$ of residue *i*-1 or *i*-3 identified from the 3D ^{15}N-separated NOESY spectrum of the S16E mutant. Wide, medium, and narrow bars represent, respectively, strong, medium, and weak NOE cross-peaks. (*B*) The correlation plot of ^{1}H-^{15}N RDCs of the S16E mutant vs. that of the WT. The correlation is 0.94 and the equation of linear regression is $y = 0.25 + 0.73x$. (*C*) Ratios of intensities of backbone amide resonances with H_2O presaturation (I_{sat}) to that without H_2O presaturation (I_{ref}). WT and S16E are represented by a blue diamond and a red square, respectively.

The S16E mutation causes subtle changes in the protein dynamics

Structural similarity does not necessarily translate into similarity in protein dynamics. The dynamic properties of the S16E mutant and the WT PLN were compared by performing standard relaxation experiments for the two proteins under identical sample and spectrometer conditions. Residue-specific ^{15}N R_1 and R_2 relaxation rates and ^{1}H-^{15}N NOEs were obtained at 30°C using the standard pulse schemes described previously in Kay et al. (1989).

Figure 3A shows that the R_2/R_1 ratios, which probe for global motion on the nanosecond timescale (Kay et al. 1989), are very similar in the WT and the mutant. In both

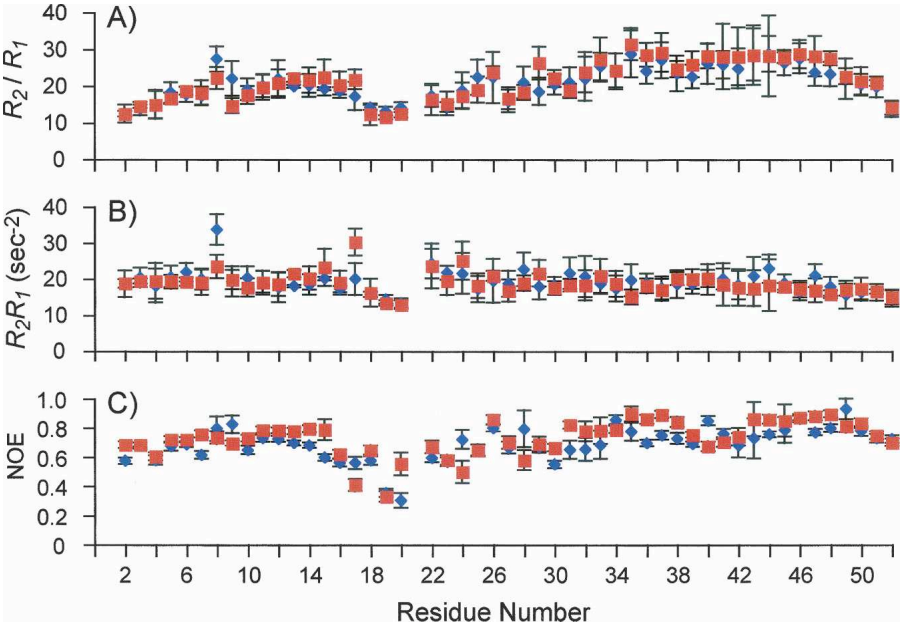

Figure 3. Characterization of the effect of the phosphorylation-mimicking mutation on the dynamic properties of the PLN pentamer. The residue-specific ^{15}N R_2/R_1 (*A*), R_2R_1 (*B*), and ^{1}H-^{15}N heteronuclear NOEs (*C*) are shown in blue for the WT and in red for the S16E mutant.

cases, the TM domain has larger R_2/R_1 ratios than the extramembrane helix, suggesting that the mobility of the extramembrane helix relative to the TM domain is present in both unphosphorylated and phosphorylated PLN. However, the R_2R_1 products, which probe for variations in the slower microsecond–millisecond chemical-exchange process (Kneller et al. 2002), reveal significant differences between the WT and the mutant at the positions of Thr8 and Thr17 (Fig. 3B). In the WT, there is larger-than-average chemical exchange associated with ^{15}N of Thr8 that is consistent with the corresponding weak and broad resonance in the TROSY spectrum (see Fig. 1A). This unusually large chemical exchange is no longer present in the S16E mutant. On the other hand, Thr17 ^{15}N has average chemical exchange in the WT, but larger-than-average chemical exchange in the mutant. The R_2R_1 products corresponding to the TM domain are essentially the same for the WT and the mutant. Finally, to examine whether the S16E mutation changes the internal dynamics of the pentamer, the ^{15}N(^{1}H) heteronuclear NOEs, which are much more sensitive to fast internal dynamics than R_1 and R_2, have been measured. Figure 3C shows that the NOEs measured for the WT and the mutant are also very similar. The average NOE value for the WT (0.68 $\pm$ 0.04) is slightly lower than that of the mutant (0.73 $\pm$ 0.04), suggesting that phosphorylation may have further stabilized the pentameric assembly.

Overall, the dynamic properties of the TM domain are not affected by the S16E mutation. The differences between the two forms of PLN are slightly larger for the extramembrane domain encompassing the extramembrane helix and the linker region connecting the helix and the TM domain. It is not clear what the implication of these differences is in the phosphorylation-regulated interaction with SERCA.

Conclusions

The structure of the PLN pentamer is not changed by the S16E phosphorylation-mimicking mutation in DPC micelles. Since replacing Ser16 with the acidic glutamate has been demonstrated to have the same effect as phosphorylation, the above result suggests that phosphorylation does not change the conformation of the pentameric assembly. The lack of differences is consistent with the above-mentioned spectroscopic studies of the effect of phosphorylation on the WT PLN pentamer (Simmerman et al. 1989; Arkin et al. 1995; Abu-Baker and Lorigan 2006). However, this result is seemingly contradictory to the report that phosphorylation of the AFA monomeric mutant causes a significant portion of the extramembrane domain (residues 14–21) to become disordered (Metcalfe et al. 2005). A plausible explanation is that the conformational stability of PLN in the pentameric form is higher than that of the monomeric AFA–PLN because helix–helix packing stabilizes the secondary structure. According to the PLN pentamer structure in DPC micelles, although the extramembrane

helices point out of the membrane into the solution, they are supported by a partially structured linker, unlike the monomeric AFA–PLN. Moreover, these helices in the pentamer can weakly interact with and support each other when taking into account their water hydration radius. Thus, the physical properties of the PLN pentamer are fundamentally different from those of the monomer.

There are some subtle differences in the dynamic properties between the mutant and the WT. These differences reside mostly in the extramembrane region of PLN encompassing the amphipathic helix and the nonhelical segment connecting the amphipathic and the TM helices. Since the extramembrane region of PLN is known to be more dynamic and important for interaction with SERCA, the subtle changes in dynamics upon phosphorylation could play a role in altering interaction with SERCA. Alternatively, it may simply be that the addition of negative charges modulates electrostatic ineractions in the PLN–SERCA complex. A high-resolution structure of such a complex will be invaluable for addressing the mechanism of SERCA regulation by PLN.

Materials and Methods

Material

Deuterated dodecylphosphocholine (DPC) is from Anatrace, Inc. ^{15}N-labeled ammonium chloride and 99% D_2O are from the Cambridge Isotope Laboratories, Inc.

Sample preparation

The genes encoding WT human PLN and the S16E mutant were cloned into the pMALc2x vector (New England Biolabs) and expressed as a maltose-binding protein (MBP) fusion protein. The detailed procedures of protein expression, purification, and reconstitution in detergent micelles are as described in Oxenoid and Chou (2005).

NMR

The sequence-specific assignment of backbone ^{1}H and ^{15}N resonances of the S16E mutant was accomplished using the 3D HNCA and ^{15}N-separated NOESY spectra acquired on ^{15}N-, ^{13}C-labeled protein, and the known assignments of the WT PLN (Oxenoid and Chou 2005). Intramonomer NOEs were assigned using the 3D ^{15}N-separated NOESY spectra recorded with NOE mixing time of 120 ms.

For RDC measurements for the S16E mutant, weak alignment of the protein–detergent complex was accomplished using a modified version (Chou et al. 2001) of the strain-induced alignment in a gel (SAG) method (Sass et al. 2000; Tckyo et al. 2000). The ^{15}N-labeled protein in DPC micelles was soaked into a cylindrically shaped polyacrylamide gel (4% acrylamide concentration and acrylamide/bisacrylamide molar ratio of 80), initially of 6 mm diameter and 9 mm length, which was subsequently radially compressed to fit within the 4.2 mm inner diameter of a NMR tube with open ends (http://newera-spectro.com), thereby increasing its length to 18 mm. The RDCs were obtained by subtracting J of the unaligned sample from $J + D$ of the aligned sample. The sign of dipolar couplings follows the convention that $|^{1}J_{NH} + {}^{1}D_{NH}| < 90$ Hz when $^{1}D_{NH}$ is positive. The ^{1}H-^{15}N RDCs were obtained from $^{1}J_{NH}/2$ and $(^{1}J_{NH} + {}^{1}D_{NH})/2$, which were measured at 600 MHz (^{1}H frequency) by interleaving a regular gradient-enhanced HSQC and a gradient-selected TROSY, both acquired with 80 ms of ^{15}N evolution.

The relative amide protection from water was measured by recording two interleaved ^{1}H-^{15}N TROSY spectra, one in the absence and the other in the presence of 1 sec of presaturation of the water resonance. The samples used for this experiment were ^{15}N-, ^{2}H-labeled WT, and S16E PLN reconstituted in deuterated DPC. The same samples were used for measurements of ^{15}N R_1, R_2, and ^{15}N(^{1}H) NOE using the standard pulse schemes described in Kay et al. (1989).

All NMR data were collected at 30°C on Bruker spectrometers operating at ^{1}H frequencies of 600 MHz and equipped with cryogenic probes. Data processing and spectra analyses were done in NMRPipe (Delaglio et al. 1995) and XEASY (Bartels et al. 1995).

Acknowledgments

This work was supported by National Institutes of Health Grant HL084329. K.O. is supported by the American Heart Association Postdoctoral Fellowship. A.J.R. is supported by the Harvard Biophysics Program and J.J.C. is supported by the Pew Scholars Program in the Biomedical Sciences.

References

Abu-Baker, S. and Lorigan, G.A. 2006. Phospholamban and its phosphorylated form interact differently with lipid bilayers: A 31P, 2H, and 13C solid-state NMR spectroscopic study. *Biochemistry* **45:** 13312–13322.

Arkin, I.T., Rothman, M., Ludlam, C.F., Aimoto, S., Engelman, D.M., Rothschild, K.J., and Smith, S.O. 1995. Structural model of the phospholamban ion channel complex in phospholipid membranes. *J. Mol. Biol.* **248:** 824–834.

Bartels, C., Xia, T., Billeter, M., Güntert, P., and Wüthrich, K. 1995. The program XEASY for computer-supported NMR spectral analysis of biological macromolecules. *J. Biomol. NMR* **6:** 1–10.

Chou, J.J., Gaemers, S., Howder, B., Louis, J.M., and Bax, A. 2001. A simple apparatus for generating stretched polyacrylamide gels, yielding uniform alignment of proteins and detergent micelles. *J. Biomol. NMR* **21:** 377–382.

Delaglio, F., Grzesiek, S., Vuister, G.W., Zhu, G., Pfeifer, J., and Bax, A. 1995. NMRPipe: A multidimensional spectral processing system based on UNIX pipes. *J. Biomol. NMR* **6:** 277–293.

Hoshijima, M., Ikeda, Y., Iwanaga, Y., Minamisawa, S., Date, M.O., Gu, Y., Iwatate, M., Li, M., Wang, L., Wilson, J.M., et al. 2002. Chronic suppression of heart-failure progression by a pseudophosphorylated mutant of phospholamban via in vivo cardiac rAAV gene delivery. *Nat. Med.* **8:** 864–871.

Huggins, J.P. and England, P.J. 1987. Evidence for a phosphorylation-induced conformational change in phospholamban from the effects of three proteases. *FEBS Lett.* **217:** 32–36.

Kay, L.E., Torchia, D.A., and Bax, A. 1989. Backbone dynamics of proteins as studied by 15N inverse detected heteronuclear NMR spectroscopy: Application to staphylococcal nuclease. *Biochemistry* **28:** 8972–8979.

Kneller, J.M., Lu, M., and Bracken, C. 2002. An effective method for the discrimination of motional anisotropy and chemical exchange. *J. Am. Chem. Soc.* **124:** 1852–1853.

Lamberth, S., Schmid, H., Muenchbach, M., Vorherr, T., Krebs, J., Carafoli, E., and Griesinger, C. 2000. NMR solution structure of phospholamban. *Helv. Chim. Acta* **83:** 2141–2152.

MacLennan, D.H. and Kranias, E.G. 2003. Calcium:Phospholamban: A crucial regulator of cardiac contractility. *Nat. Rev. Mol. Cell Biol.* **4:** 566–577.

Metcalfe, E.E., Traaseth, N.J., and Veglia, G. 2005. Serine 16 phosphorylation induces an order-to-disorder transition in monomeric phospholamban. *Biochemistry* **44:** 4386–4396.

Oxenoid, K. and Chou, J.J. 2005. The structure of phospholamban pentamer reveals a channel-like architecture in membranes. *Proc. Natl. Acad. Sci.* **102:** 10870–10875.

Park, K.S., Mohapatra, D.P., Misonou, H., and Trimmer, J.S. 2006. Graded regulation of the Kv2.1 potassium channel by variable phosphorylation. *Science* **313:** 976–979.

Sass, H.J., Musco, G., Stahl, S.J., Wingfield, P.T., and Grzesiek, S. 2000. Solution NMR of proteins within polyacrylamide gels: Diffusional properties and residual alignment by mechanical stress or embedding of oriented purple membranes. *J. Biomol. NMR* **18:** 303–309.

Simmerman, H.K., Lovelace, D.E., and Jones, L.R. 1989. Secondary structure of detergent-solubilized phospholamban, a phosphorylatable, oligomeric protein of cardiac sarcoplasmic reticulum. *Biochim. Biophys. Acta* **997:** 322–329.

Stokes, D.L., Pomfret, A.J., Rice, W.J., Glaves, J.P., and Young, H.S. 2006. Interactions between Ca^{2+}-ATPase and the pentameric form of phospholamban in two-dimensional co-crystals. *Biophys. J.* **90:** 4213–4223.

Tckyo, R., Blanco, F.J., and Ishii, Y. 2000. Alignment of biopolymers in strained gels: A new way to create detectable dipole-dipole couplings in high-resolution biomolecular NMR. *J. Am. Chem. Soc.* **122:** 9340–9341.

Toyoshima, C. and Nomura, H. 2002. Structural changes in the calcium pump accompanying the dissociation of calcium. *Nature* **418:** 605–611.

Toyoshima, C., Asahi, M., Sugita, Y., Khanna, R., Tsuda, T., and MacLennan, D.H. 2003. Modeling of the inhibitory interaction of phospholamban with the Ca^{2+} ATPase. *Proc. Natl. Acad. Sci.* **100:** 467–472.

Yang, Y., Craig, T.J., Chen, X., Ciufo, L.F., Takahashi, M., Morgan, A., and Gillis, K.D. 2007. Phosphomimetic mutation of Ser-187 of SNAP-25 increases both syntaxin binding and highly Ca^{2+}-sensitive exocytosis. *J. Gen. Physiol.* **129:** 233–244.

Zamoon, J., Mascioni, A., Thomas, D.D., and Veglia, G. 2003. NMR solution structure and topological orientation of monomeric phospholamban in dodecylphosphocholine micelles. *Biophys. J.* **85:** 2589–2598.

Zucchi, R. and Ronca-Testoni, S. 1997. The sarcoplasmic reticulum Ca^{2+} channel/ryanodine receptor: Modulation by endogenous effectors, drugs and disease states. *Pharmacol. Rev.* **49:** 1–51.